Carbon 215 (2023) 118483

Contents lists available at ScienceDirect

Carbon

journal homepage: www.elsevier.com/locate/carbon

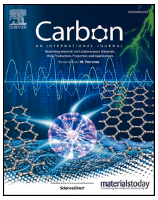

Molten salt carbon felt oxidation for VRFB electrode performance improvement

Justyna Piwek [a], Gabriel Gonzalez [b], Pekka Peljo [b,**], Elzbieta Frackowiak [a,*]

[a] Poznan University of Technology, Institute of Chemistry and Technical Electrochemistry, Berdychowo 4, Poznan, 60-695, Poland
[b] University of Turku, Department of Mechanical and Materials Engineering, Research Group of Battery Materials and Technologies, Vesilinnantie 5, Turku, FI-20014, Finland

ARTICLE INFO

Keywords:
Carbon felt oxidation
Vanadium redox flow battery
Molten salt electrode treatment

ABSTRACT

In this study, carbon felt (CF) electrodes were chemically treated using alkali metal salt (potassium nitrate) in the molten state as a mild oxidizing agent. Various temperatures in the range of 380–500 °C and oxidation duration (up to 12 h) were analyzed in order to find the most appropriate oxidation conditions. As-prepared carbon felts were electrochemically investigated in a three-electrode set-up as well as in a lab-scale vanadium redox flow battery (VRFB). The battery set-up included additional *in-situ* potential measurements allowing to measure the polarization of each electrode separately and compare the performance of heat- and chemically-treated electrodes. The physico-chemical properties of CFs have been analyzed using X-ray photoelectron spectroscopy (XPS) and other advanced techniques. Combination of extended oxidation time with temperature increase causes satisfactory surface functionalization and enhanced vanadium redox reaction reversibility. The chemically treated samples showed a better performance with lower overpotentials and higher efficiencies. Improved reversibility of V^{2+}/V^{3+} reaction is obtained for the carbon felt treated with salt presence. What is more, a 4 times reduced CF electrode oxidation time as usually presented in literature (12 h for heat-treated electrodes *vs.* 3 h for salt- and heat-treated ones) can be achieved with nitrate salt oxidation.

1. Introduction

Over the last few years, the interest about the redox flow battery technology notably increased due to significant activity towards energy storage from renewable sources (wind, sun). Redox flow batteries (RFBs) are energy conversion systems mainly used for stationary applications. Their distinctive properties allow the energy and power to be decoupled. The power of RFB is bound to the size and number of electrochemical cells in the stack, whereas energy is governed by electrolyte (active species concentration and electrolyte volume). Therefore, RFBs are a perfect approach for large scale application since their final output can be easily adjusted and thus are able to deliver relatively high energy [1].

Several novel RFB chemistries have been already developed, however, their improvements are essential for commercial application. One of the most popular RFB system is vanadium redox flow battery (VRFB) which is a rechargeable battery that utilizes all vanadium oxidation states. V^{2+}/V^{3+} and VO^{2+}/VO_2^+ redox pairs are used for the negative and positive side, respectively [2]. In VRFB, vanadium is dissolved in a supporting electrolyte (usually 1–3 mol L^{-1} sulfuric acid) with a maximum concentration of 1–2 mol L^{-1} [3].

The following reactions takes place during discharging processes:

$$\text{Positive side}:\ VO_2{}^+ + e^- + 2H^+ \leftrightarrow VO^{2+} + H_2O,\ E^0 = 1.004\ V$$

$$\text{Negative side}:\ V^{2+} \leftrightarrow V^{3+} + e^-,\ E^0 = -0.255\ V$$

$$\text{The overall reaction}:\ VO_2{}^+ + 2H^+ + V^{2+} \leftrightarrow VO^{2+} + H_2O + V^{3+},\ E^0 = 1.259\ V$$

The standard battery voltage (at 25 °C and 1 mol L^{-1} concentration) equals to 1.259 V and stands as the difference between positive and negative half-cells.

The electrodes for redox flow batteries application have a different role than in the conventional secondary batteries. Most importantly, they do not undergo through any reaction by themselves, however, they provide a platform for vanadium redox reaction that occurs on electrode

---

* Corresponding author.
** Corresponding author.

E-mail addresses: pekka.peljo@utu.fi (P. Peljo), elzbieta.frackowiak@put.poznan.pl (E. Frackowiak).

https://doi.org/10.1016/j.carbon.2023.118483
Received 29 July 2023; Received in revised form 22 September 2023; Accepted 23 September 2023

surface. Secondly, the electrodes should serve as channels for electrolyte that has to flow through the electrode. Therefore, porous, three-dimensional structure is an essential requirement for RFB electrodes to provide a uniform distribution of the electrolyte [4].

Development of the ideal electrode for redox flow battery application is one of the current research challenges. To meet above-mentioned requirements intensive studies have been carried out. To date, various electrode materials have been developed including carbon-based materials, conductive plastics (carbon-polymer composites), metals and metallic oxides [4–6]. It was found out that carbon-polymer composites suffer from poor electrochemical activity due to low conductivity and low surface area [7]. Some of composites with high-carbon loadings are quite acceptable, however, results of Skyllas-Kazacos et al. indicate that carbon-impregnated current collectors can improve energetic efficiency of VRFB [8]. High electrochemical activity is presented by all the metallic materials usually based on precious metals (Au, Ir, Pt, Ru) or their oxides. Yet, their high costs, short-term stability and electrocatalytic activity towards oxygen/hydrogen evolution reaction (e.g., dimensionally stable anode (DSA) with IrO_2 nanoparticles) exclude them from practical applications [4].

Carbon felts (CF) are commonly used electrodes for VRFB because of their stability in acidic solution, wide potential window, flow through porous texture and low cost [3,5,9].

Nevertheless, they still possess some disadvantages, which limit VRFB proper long-term performance. Even though VRFBs are already commercialized, there are still some issues which could be improved. This mainly concerns carbon corrosion or oxygen/hydrogen evolution side reactions on the positive/negative side, respectively. It was observed that some side reactions may lead to VRFB performance fading. Since, V^{2+}/V^{3+} redox pair operates at $E^0 = -0.255$ V vs. SHE, H_2 evolution is a competitive reaction on the negative side of VRFB which leads to electrolyte pH and concentration change [10,11]. Moreover, carbon corrosion and oxygen evolution reaction on the positive side of VRFB cause battery performance losses over time [12]. Therefore, it is essential to develop a material with good electrical conductivity and proper activity to improve overall RFB properties. This can be realized *via* CF functionalization with oxygen- or nitrogen-surface groups. The optimization of electron transfer process at the carbon electrode surface is still under intensive development, however, many solutions include quite expensive materials and high-tech processes. Without a doubt, carbon felt surface modification is necessary [13–16]. It includes various oxidation methods with the most recognized and used industrially one – heat-treatment at oxidative atmosphere [17–19]. Some other studies include utilization of CF electrodes with noble metals, carbon nanotubes and many alternative-effective oxidation methods [17,20,21]. Various carbonaceous materials including carbon felts (CFs), graphite felts (GFs), carbon papers (CPs), carbon nanotubes (CNTs), and graphite are applied. CFs and GFs are indeed mostly used electrodes for VRFB application. It was demonstrated by Skyllas-Kazacos et al. that polyacrylonitrile (PAN)-based GF performance has much suitable characteristics than Rayon (cellulose) fibers [22]. Interestingly, utilization of CP can reduce the resistance in VRFB, however, to ensure high enough surface area, it is recommended to use three layers of CP in a battery cell [23]. Thermal-treatment of CFs and GFs represents a straightforward, cost-effective, and minimally resource-intensive method for surface modification. As early as 1992, the research team led by Skyllas-Kazacos et al. conducted an examination of the characteristics of GFs subjected to different temperatures and durations of treatment. The ideal temperature for enhancing the wettability and conductivity of GF was identified as 400 °C [24]. This temperature led to significant improvement in GF properties. These beneficial changes in GF characteristics were achieved through the incorporation of oxygen-functional groups, specifically C═O and C–OH, which serve as active sites for the vanadium oxidation/reduction reaction. X-ray photoelectron spectroscopy (XPS) analyses demonstrated that phenolic groups (C–OH) primarily influenced the electrochemical performance of VRFBs. The presence of oxygen-rich groups on the carbon surface plays a crucial role in enabling the reversible vanadium redox reaction. Various investigations have addressed the thermal treatment of GFs. For instance, Park et al. proved that a gentle oxidation process for carbon felts at 500 °C for 5 h can enhance the energetic efficiency of VRFBs, even after 500 cycles [25,26]. Schweiss et al. noticed a parasitic hydrogen evolution on the negative side of RFB battery for Rayon and PAN-based carbon felts before and after the thermal treatment at 750 °C for 5 min [27]. All the studies performed claim that one of the main reasons for RFB performance fade is the degradation of electrodes due to side reactions [28,29]. It comes from irreversible hydrogen evolution which occurs at potentials close to V^{2+}/V^{3+}. Additionally, at positive side, carbon corrosion connected with CO_2 and CO evolution takes place. As degradation occurs, surface functional groups are slowly eliminated, potentially leading to a reduction in the electrochemically active surface area [30,31]. R. Zeiss et al. investigated the influence of thermal treatment as well as soaking in H_2SO_4 on commercially available GFs. They proved that chemical treatment has a stronger impact on thermal stability of PAN felts. Furthermore, it was shown that the thermal stability after heat-treatment is lower for carbonized felts compared to graphitized ones. What is more, it was proven by TGA-MS that soaking and electrochemical ageing lead to a much lower thermal stability for all felt type and aged carbons are more prone to side reactions [32]. Importantly, it is also recommended to activate carbon-based electrodes just before battery operation [33]. Not only the oxygen surface groups play an important role in RFB performance. Introduction of nitrogen surface groups improves the electrochemical kinetics of vanadium reaction as well as higher energetic efficiency of RFB is recorded. An alternative nitrogen-doping technique is based on the *in-situ* polymerization of polypyrrole, followed by carbonization in a $Co(NO_3)_2$ solution. This nitrogen-doped graphene framework demonstrated enhanced electrochemical kinetics for vanadium reactions [34]. Certain studies have reported that ammonia, either alone or in combination with oxygen, can lead to the formation of a notably functionalized carbon surface. PAN-based graphite electrodes treated with a 1:1 mixture of NH_3:O_2 for 5 h at the temperature of 700 °C exhibited nitrogen and oxygen content levels of approximately 8% and 32%, respectively. Co-doping of both nitrogen and oxygen exhibits a synergistic effect, which significantly enhances the redox reactions of vanadium ions compared to doping with either oxygen or nitrogen atoms individually [35]. Performance enhancement of graphite felt was also made by incorporating sulfur/-nitrogen (S/N) co-doped quantum dots. The introduction of these S/N co-doped quantum dots resulted in improved catalytic activity, overall electrode efficiency, and battery durability [36]. Dixon et al. employed N_2 plasma treatment to modify PAN-based carbon felt. This treatment not only introduced nitrogen doping but also enhanced the presence of edge defects by eliminating aliphatic functional groups from the surface of carbon fibers [37]. Kim et al. fabricated nitrogen-doped graphite felt using melamine as the nitrogen source. Their findings indicated that oxygen functional groups present on the surface of the graphite felt positively influenced the incorporation of nitrogen [38].

All these studies emphasize the connection between the electrochemical performance of VRFBs and the characteristics of reaction sites, such as the types and quantity. Therefore, it is essential to find a trade-off between the amount and type of introduced species and the VRFB performance, especially taking into account the lifespan of cell and the cost of the proposed method. Functionalization of carbon material by oxygen/nitrogen is crucial to achieve the redox reaction reversibility during charging/discharging of the battery. It can be realized *via* adaptation of various carbon electrode oxidation methods while retaining the high conductivity. Therefore, our research is focused on the development of relatively inexpensive and facile method for carbon felt surface oxidation using potassium nitrate salt in a molten state. Both physico-chemical and electrochemical studies allow CF surface properties with the vanadium redox reaction behavior to be correlated and in effect VRFB operation was improved. The samples treated thermally with salt presence revealed an improved performance with lower overpotentials and higher efficiencies. A detailed analysis of cyclic voltammetry proved better reversibility of V^{2+}/V^{3+} reaction while the electrode preparation time was reduced by a factor of 4.

2. Experimental

2.1. *Carbon felt modification*

Two various carbon felt electrodes (GFD 4.6 and KFD 2.5) from SGL Carbon company (Germany) were used for surface modification. Carbon felt electrodes were firstly pre-activated chemically in concentrated nitric acid (HNO_3) for 48 h. Afterwards, the materials were cleaned with distilled water, ethanol and dried in 60 °C. As prepared electrodes were further treated with alkali metal salt in a molten state. Carbon felt was placed in the ceramic crucible and potassium nitrate salt was spread evenly around the sample. The amount of the KNO_3 salt utilized is equal to 0.6 g per 1 cm^2 of carbon felt. The melting temperature of KNO_3 salt equals to 334 °C [39]. The samples were heat-treated with the presence of KNO_3 salt in various conditions (380–440 °C) for 10 min in ambient atmosphere (samples are named according to the heat treatment temperature e.g., GFD/KFD-380). Moreover, the samples treated at 500 °C for 3–12 h with and without salt were compared. To fully understand each step of oxidation process, samples treated in acid only (without salt) or in salt only (without acid pre-treatment) were prepared. Tube furnace (Shinko company) was applied for heating. After the treatment, all the CFs were washed extensively with distilled water in ultrasonic bath and dried again.

2.2. *Electrochemical characterization*

a) Three-electrode measurements

The CF samples were tested electrochemically in a three-electrode cell set-up. Carbon felt electrodes played a role of the working electrode with the diameter of 10 mm. Pt mesh was applied as the counter electrodes, whereas Hg/Hg_2SO_4 in 2 mol L^{-1} H_2SO_4 was a reference electrode with $E^0 = 0.674$ *vs.* SHE. Titanium current collectors were used. 0.1 mol L^{-1} $VOSO_4$ solution in 2 mol L^{-1} H_2SO_4 was the electrolytic medium. The samples were tested using cyclic voltammetry at 2 mV s^{-1}. Both vanadium redox pairs, i.e., V^{2+}/V^{3+} and VO^{2+}/VO_2^+ were studied. The electrochemical performance for three-electrode set-up was measured by a multichannel VMP3 potentiostat/galvanostat with EC-Lab software from Biologic® (France).

b) VRFB study including electrodes *in-situ* polarization measurements

The performance of the treated carbon felts was tested in a lab-scale VRFB. The experimental set-up includes an extra cell after the main one that allows recording the potential difference between two carbon plates i.e., the open circuit potential (OCP). Then, the electrolytes flow from the reservoirs to the main cell and, after that, to the OCP-cell and back to the tanks. This set-up records the polarization of each electrode separately by measuring the potential difference between the carbon plate of the main cell against the carbon plate of the OCP-cell for both negolyte and posolyte. A scheme of the set-up is shown in Fig. 1.

The performance of the treated carbon felts was tested when cycling at different current densities: 25, 50, 75 and 100 mA cm^{-2} (6 cycles per current density). The cut-off voltages were 1.70 V and 0.90 V for charge and discharge, respectively. The experiments were performed with a Pinflow standard single cell with a membrane (Nafion® 117) area of 20 cm^2. 50 ml of a commercial vanadium electrolyte solution (1.6 mol L^{-1} of vanadium in 2 mol L^{-1} H_2SO_4) from Gesellschaft für Elektrometallurgie mbH (GfE) was used on each side. The cycling was performed with a constant flow rate of 100 ml min^{-1} at room temperature. In order to minimize the amount of oxygen in the system, nitrogen was bubbled to the reservoirs during the experiments. The measurements were recorded using a LANHE Battery Testing System G340A. Additionally, potential electrochemical impedance spectroscopy (PEIS) was performed at OCP in the frequency range 10 kHz–1 Hz for the main cell before starting the cycling. The measurements were performed using a SP-240 potentiostat from Biologic® (France) with EC-Lab software.

c) Physico-chemical characterization

Additionally, physico-chemical properties of carbon materials were

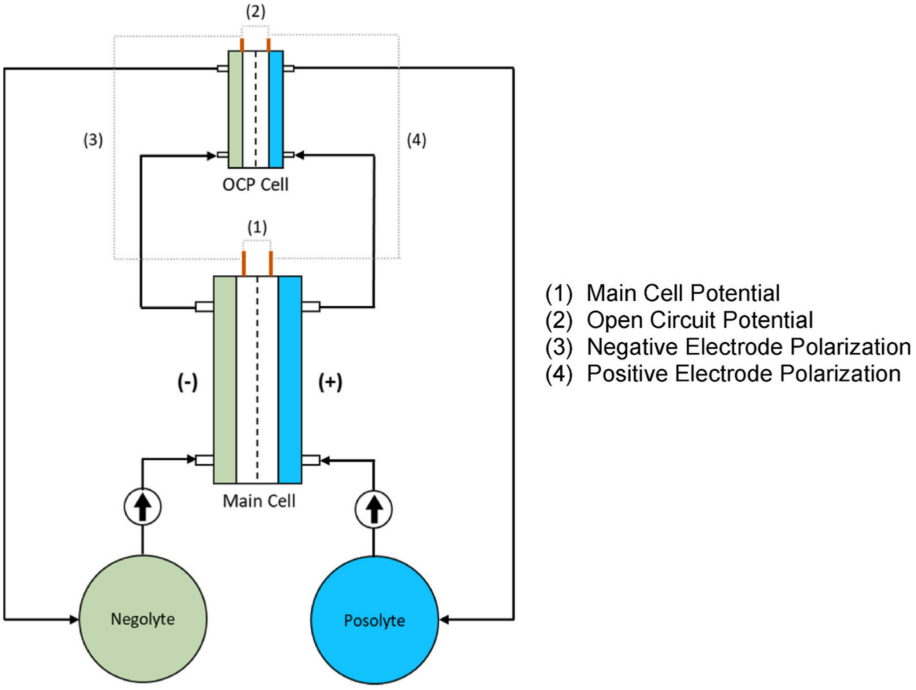

Fig. 1. Scheme of VRFB experimental set-up and *in-situ* potential measurements. (A colour version of this figure can be viewed online.)

studied using X-ray photoelectron spectroscopy (XPS) and contact angle measurements. For water uptake measurements, carbon felt samples were soaked with 0.1 mol L^{-1} $VOSO_4$ in 2 mol L^{-1} H_2SO_4 for 30 s at room temperature. The water uptake (WU) was calculated according to the formula:

$$WU = \frac{W_w - W_D}{W_D}$$

where: W_W - sample weight after absorption [g]; W_D - sample weight before absorption [g].

The surface texture was examined using scanning electron microscopy (Hitachi Model S-3400 N) with a quad-type semiconductor backscattered electron (BSE) detector.

The XPS analyses were carried out in a PHI VersaProbeII Scanning XPS system using monochromatic Al Kα (1486.6 eV) X-rays focused to a 100 μm spot and scanned over the area of 400 μm × 400 μm. The photoelectron take-off angle was 45° and the pass energy in the analyzer was set to 117.50 eV for survey scans and 46.95 eV to obtain high energy resolution spectra for the C 1s, N 1s, K 2p and O 1s regions. A dual beam charge compensation with 7 eV Ar^+ ions and 1 eV electrons were used to maintain a constant sample surface potential regardless of the sample conductivity. At least two independent spots were analyzed at each sample. All XPS spectra were charge referenced to the unfunctionalized, saturated carbon (C–C) C1s peak at 284.8 eV. The operating pressure in the analytical chamber was less than 3×10^{-9} mbar. Deconvolution of spectra was carried out using PHI MultiPak software (v.9.9.0.8). Spectrum background was subtracted using the Shirley method.

The conductivity of the carbon felt electrodes was measured using custom-made constant force four point resistance measurement setup. The conductivity was calculated according to the formula:

$$\rho = \frac{R \bullet A}{h}$$

$$\sigma = \frac{1}{\rho}$$

where: h – thickness [m], ρ – resistivity [Ω m], R – resistance [Ω], A – area [m^2] σ – conductivity [S m^{-1}].

The contact angle measurements of carbon felts were performed with a computer-controlled goniometer (Dataphysics® OCA).

3. Results and discussion

The properties of carbon felt from SGL Carbon are presented in Table 1, while their preparation scheme is shown in Fig. 2. Both carbon felts (CFs) are made from the same precursor, i.e., PAN (polyacrylonitrile). The details about their preparation are not accessible since it covers company 'know-how'. However, thermal activation for pristine material is necessary [40]. KFD carbon felt is a carbonized material while GFD is a graphitized one. GFD has better conductivity and chemical resistivity compared to KFD carbon felt.

Table 1
Properties of studied carbon felts [40].

Properties	Carbonized felt (KFD 2.5 EA)	Graphitized felt (GFD 4.6 EA)
Fiber precursor	PAN	PAN
Nominal thickness, mm	2.5	4.6
Chemical resistivity	+	+++
Compressibility	+	+
Bulk density, g cm^{-3}	0.1	0.09
Area weight, g cm^{-3}	250	465
Open porosity, %	>90	94
S_{BET}, m^2 g^{-1}	0.6	0.4
Total impurities, %	<0.6	<0.05
Costs	+++	+

The comparison between two various CFs is presented in Fig. 3. Cyclic voltammetry for the full scan (2 mV s^{-1}) clearly shows that KFD carbon felt reveals more capacitive character than graphitized one, which may relate to a slightly higher specific surface area than GFD (Table 1). Both CFs were subjected to pre-oxidation process with nitric acid in order to pre-activate the surface for further oxidation. As seen from Fig. 3, when the acid-treatment was applied, both cyclic voltammograms become narrower, suggesting CFs oxidation and therefore, slightly more resistive character. Herein, for performance comparison, the CV scans were carried out in full range of vanadium working potential (from −0.5 to 1.3 V vs. SHE). However, for the following measurements, carbon felt behavior in V^{2+}/V^{3+} and VO^{2+}/VO_2^+ will be analyzed separately to simulate the processes in VRFB.

To prove the necessity of carbon felt-surface pre-treatment with HNO_3, further electrochemical measurements coupled with XPS studies were carried out (Fig. 4). As seen from Fig. 4A, vanadium reactions are almost inactive for pristine CF. When the oxidation is applied, one can observe respective oxidation/reduction peaks of vanadium species. Usually, reduction of VO^{2+} to V^{3+} is not visible due to its poor reversibility [18,41]. However, when both acid and salt were used, the peak separation is smaller and more reversible processes are recorded. Pristine GFD carbon possess 2.1 at. % of oxygen and 97.9 at.% of carbon. When both salt and acid treatment were carried out, oxygen content doubled (5 at. %), whereas 3 at. % is obtained for salt-treated only sample. Therefore, it is proven by XPS studies that enhancement of oxidation is obtained with acid pre-treatment. As shown in deconvoluted XPS spectra (Fig. 4B), two types of oxygen groups can be distinguished and salt treatment only enhances already present surface groups without introducing the novel ones.

Fig. 5 presents SEM micrographs of differently prepared GFD samples. One can observe that carbon felt consists of individual fibers. Oxidation process adapted for these studies does not significantly influence the texture of studied samples; slight thickness reduction is visible for the samples with the salt presence. It can be therefore assumed that non-aggressive conditions are used; mild oxidation *via* salt treatment is assumed.

Firstly, the carbon felt treatment in the presence of salt was carried out at the various temperatures (380–440 °C) for 10 min. Herein, two redox couples (V^{2+}/V^{3+} and VO^{2+}/VO_2^+) were studied separately by voltammetry. Cyclic voltammetry profile (2 mV s^{-1}) was recorded at two various potential ranges (Fig. 6A). When the negative side (V^{2+}/V^{3+}) is considered, one can observe that GFD-380 and GFD-400 are almost inactive and cyclic voltammograms resemble the shape of the pristine sample. Treatment at 380 °C does not ensure a homogenous salt distribution. When 400 °C was used, the CF response is quite good for positive side (VO^{2+}/VO_2^+), however, it is still too low temperature for the negative side to be improved. It can be also seen that with an increase of temperature, a higher vanadium reversibility is obtained. To observe the surface changes over various treatment conditions, XPS spectra were collected. As presented in Fig. 6B, none of the samples, except GFD-380, contains nitrogen on its surface. Moreover, higher oxygen content than expected (not in trend) was detected for GFD-380. These facts indicate that GFD-380 was not washed enough and some traces of NO_3^- remained on its surface. Moreover, it was observed that the salt at 380 °C is scattered in points on CF surface (non-equal salt distribution) causing there a higher oxidation state. For all other samples the trend is linear – oxygen content increases with the increased treatment temperature. The highest oxygen content is obtained for GFD-440 (6.8 at.%). Additionally, the water uptake was measured for each sample to estimate its hydrophilicity. Water uptake value increases linearly with temperature meaning that a higher wettability is obtained for treated samples (Fig. 6C).

Based on obtained electrochemical data, vanadium peak analysis was carried out. Two factors were elucidated, i.e., peak potential difference (ΔE) and peak current ratio (ΔI). Both parameters allow the

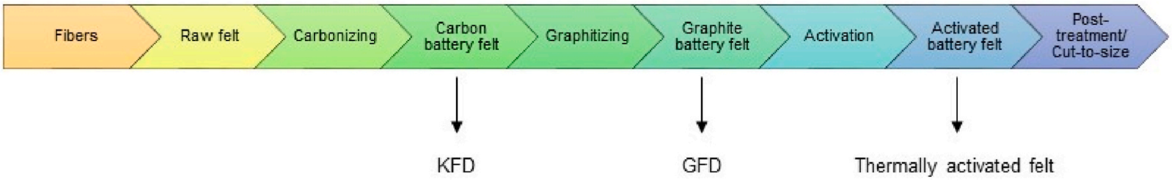

Fig. 2. Scheme of carbon felt preparation method [40]. (A colour version of this figure can be viewed online.)

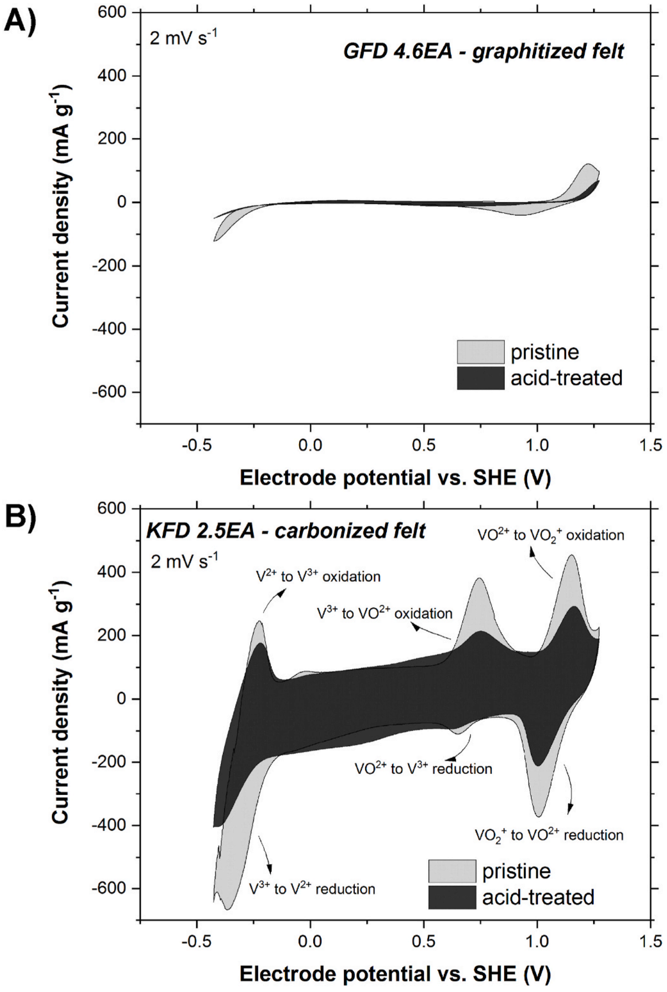

Fig. 3. Cyclic voltammetry profiles (2 mV s^{-1}) for pristine and acid-treated carbon felts A) GFD; B) KFD. Electrolytic solution – 0.1 mol L^{-1} VOSO$_4$ in 2 mol L^{-1} H$_2$SO$_4$.

redox reaction reversibility to be analyzed. When ΔE is smaller and ΔI is closer to 1, a higher reversibility can be assumed. Fig. 7 presents the data for differently treated GFD samples. When the negative side (V^{2+}/V^{3+}) is considered, one may notice that GFD-380 performs practically as the pristine sample. The reversibility increases dramatically from 400 °C and the best one is obtained for GFD-420 (ΔE = 0.19 V; ΔI = 2.8). It is worth highlighting that it is always harder to optimize the negative side of VRFB, since V^{2+} is sensitive to oxygen presence and the reaction compete with hydrogen evolution. Therefore, the results presented for the positive side (Fig. 7C and D) have better ΔE and ΔI parameters. Herein, the vanadium reaction reversibility increases linearly with temperature rise. GFD-440 is the most appropriate for VO^{2+}/VO_2^+ side revealing ΔE = 0.22 V and ΔI = 0.86. These results can be directly connected with oxygen content increase above presented in Fig. 6B. All the electrochemical and physico-chemical data are also consistent with water uptake values (Fig. 6C), which refer to the ratio of absorbed water weight to dry material weight.

Similar analysis of peak response was performed for KFD carbon felt. As above-mentioned, KFD carbon felt is not rigid and as stable as GFD one and its thermal stability is lower. Therefore, the molten salt treatment was only performed at 380 °C and 400 °C. 420 °C is already beyond KFD stability limit. Fig. 8 presents cyclic voltammograms and surface composition from XPS measurements recorded for KFD samples. It can be observed that the trend is opposite to GFD; higher current response is recorded for KFD-380 and only slight improvement for KFD-400 is noticed when compared to pristine carbon. This observation is confirmed during peak analysis (Table 2). An excellent reversibility of KFD-treated samples may be also connected with its surface composition (Fig. 8B). Contrary to GFD felt, KFD contains pristine nitrogen and higher oxygen content. Therefore, KFD sample is more hydrophilic and more sensitive to molten-salt treatment. As seen in Fig. 8B, the treatment with KNO_3 salt may enhance nitrogen content in KFD sample from 3.7 at. % (pristine) to 6.1 at. % (KFD-380 and KFD-400). Interestingly, slightly higher oxygen content is obtained for KFD-380 than for KFD-400 and therefore it is assumed that KFD-380 reveals better peak parameters (ΔE and ΔI).

As presented in the above paragraphs, electrode treatment has to be adapted to the specific electrode type. KFD carbonized carbon felt is less stable in higher temperatures and the proposed treatment goes above its stability. Moreover, oxygen content of KFD felt is initially two times higher than for GFD one which makes it more hydrophilic as well as more fragile to any thermal and/or chemical treatment. As known, carbonized felt (KFD) is also less conductive. Therefore, for further analysis an exploration of molten salt oxidation method is performed only for graphitized (GFD) carbon felt which is more conductive, stable and prone to oxidation. What is important, the results recorded for KFD series proved a positive influence of nitrogen presence on vanadium redox reaction behavior. Therefore, our motivation was to introduce also the nitrogen to carbon structure and find the trade-off between oxygen, carbon and nitrogen content to ensure a reversible vanadium behavior. Moreover, it was shown that temperature has a crucial influence on CF final performance. For GFD carbon felt there is still a room for improvement, the next part of the research concerns GFD further treatment. Samples were heated with and without salt at 500 °C for 3–12 h named, e.g., 3 h HT (heat treatment only) and 3 h HT + ST (heat treatment with salt presence). The temperature between 450 and 500 °C is usually recommended by SGL Carbon to activate GFD felt. It also allows introducing nitrogen as well as an optimal content of oxygen on the carbon structure, as will be shown in the results below.

The mass of carbon felt was controlled during each treatment process. For comparison the felt circles of 10 mm were cut and the mass was estimated from 3 various samples. On this basis, the burn-off percentage was calculated for each sample. As observed in Table 3, the mass of only heat-treated samples does not change over the oxidation process independently on time. Nevertheless, for salt treated carbon felts the mass decreased by 15% already after 3 h. For 12 h HT + ST sample, the oxidation time caused a significant mass loss up to ca. 67% suggesting that these conditions are already too destructive. This sample is very fragile and it is impossible to prepare relatively big electrodes (only 10 mm diameter pieces). Therefore, for VRFB full system measurements, 12 h HT + ST sample is excluded.

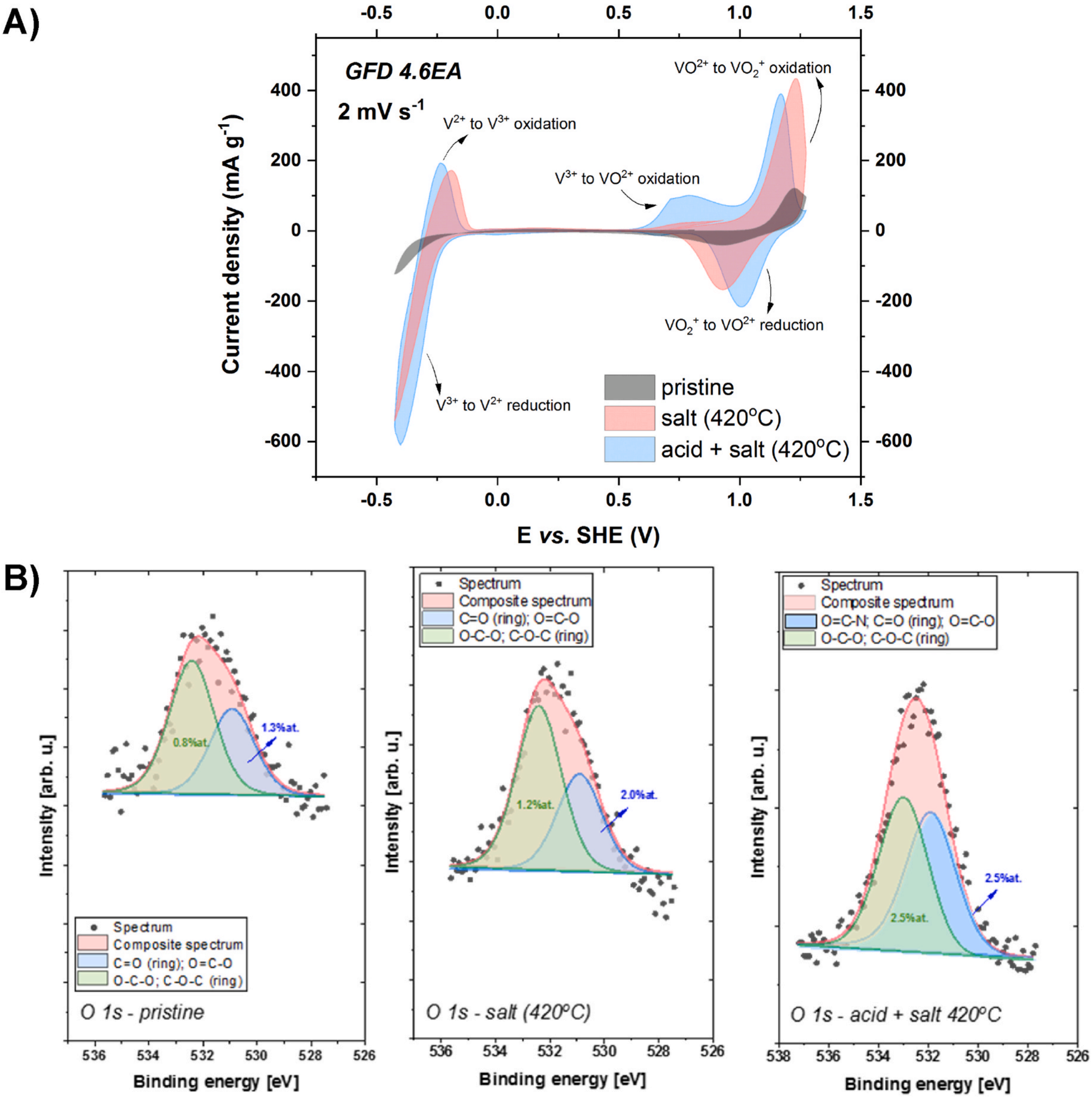

Fig. 4. Influence of carbon acid pre-treatment: A) cyclic voltammetry (2 mV s^{-1}) in the potential range −0.4-1.3 V vs. SHE; B) O1s XPS spectra. (A colour version of this figure can be viewed online.)

Moreover, the conductivity of each sample was measured (Fig. 9). The pristine GFD 4.6 EA carbon felt has the highest conductivity (241 S m^{-1}). Upon oxidation process its conductivity decreases. Nevertheless, this process is necessary to introduce surface functional groups to the carbon structure and ensure oxygen vacancies for reversible vanadium oxidation-reduction process in VRFB system. One may observe that while oxidation time increases, the conductivity decreases. However, for heat treatment process the differences are relatively small (164 S m^{-1} vs. 150 S m^{-1} for 3 h HT and 12 h HT). When the salt is present, the conductivity of 3 h HT + ST samples is comparable to heat treated samples, but decreases drastically to 35 S m^{-1} for 12 h HT + ST sample. This proves our assumption that 12 h oxidation time with salt presence is already too destructive for carbon felt. Evidently, the salt presence enhances the oxidation process and this aspect will be further discussed with electrochemical data evaluation.

In order to support previous statements, the wettability of each sample was measured using drop sessile method. The contact angle for GFD 4.6 A (pristine) is equal to 145°. Upon heat treatment it decreases to 135° and 130° for 3 h HT and 6 h HT, respectively. When the 12 h HT process was adapted, the samples change completely and become hydrophilic, and it was impossible to measure contact angle since the liquid soaked into the sample immediately. Interestingly, all HT + ST samples are strongly hydrophilic.

The electrochemical response of salt treated GFD samples is presented in Fig. 10. When the positive side of VRFB is considered, one may observe that both the recorded current density and the reversibility of VO^{2+}/VO$_2^+$ decrease with increasing treatment time. The CV curve for 3 h HT + ST sample presents very sharp, well developed redox peak with the smallest peak separation potential ($\Delta E = 0.11$ V for 3 h HT + ST vs. $\Delta E = 0.22$ V for 12 h HT + ST). An interesting behaviour is observed at the negative side. Similarly, as for VO^{2+}/VO$_2^+$ 3 h of treatment is the most appropriate carbon felt oxidation condition. However, the highest current response for oxidation process is recorded for 6 h HT + ST sample. Interestingly, quite good electrochemical response is recorded for 12 h of HT + ST sample. Though, as above-mentioned this CF is too much oxidized and its mechanical properties are too fragile to adapt salt treatment oxidation process in a bigger scale.

In order to support the obtained electrochemical data, the XPS

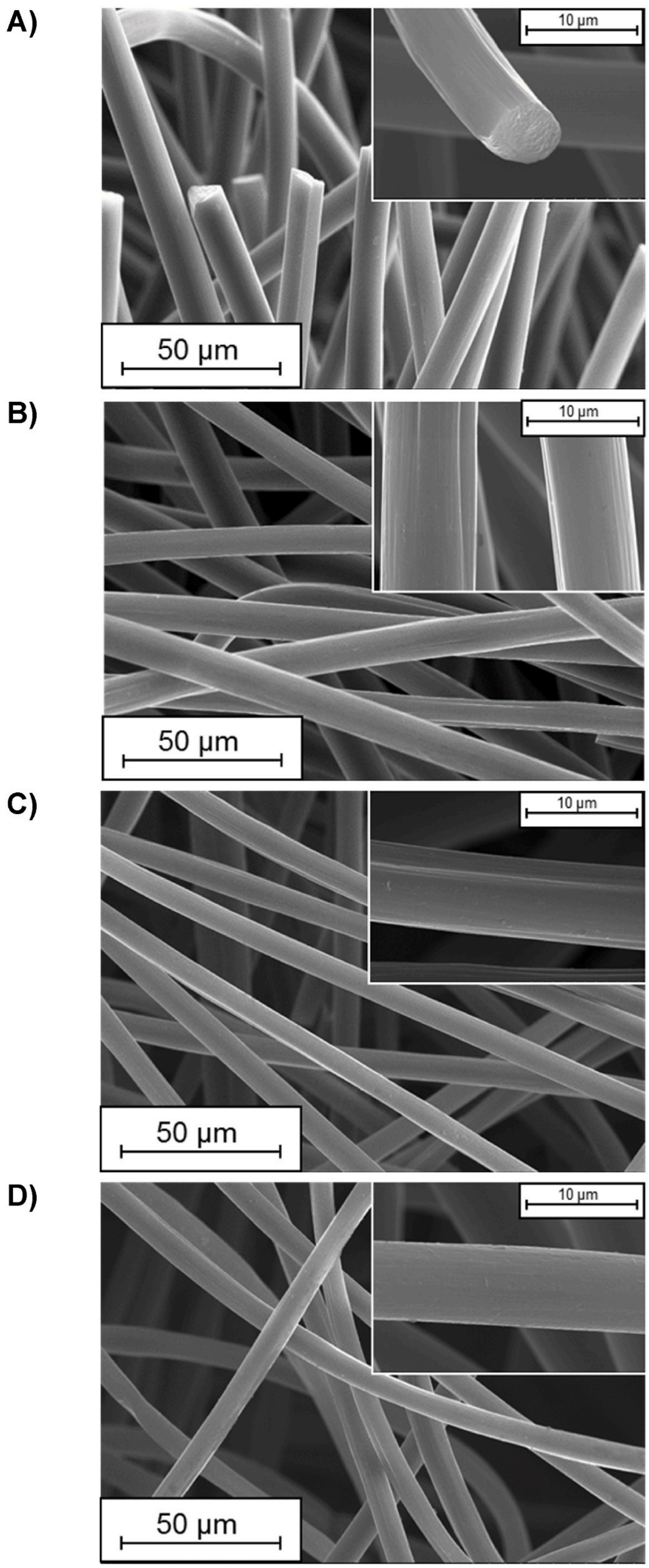

Fig. 5. SEM micrographs of GFD carbon felt: A) pristine; B) acid-treated; C) salt-treated; D) acid & salt-treated.

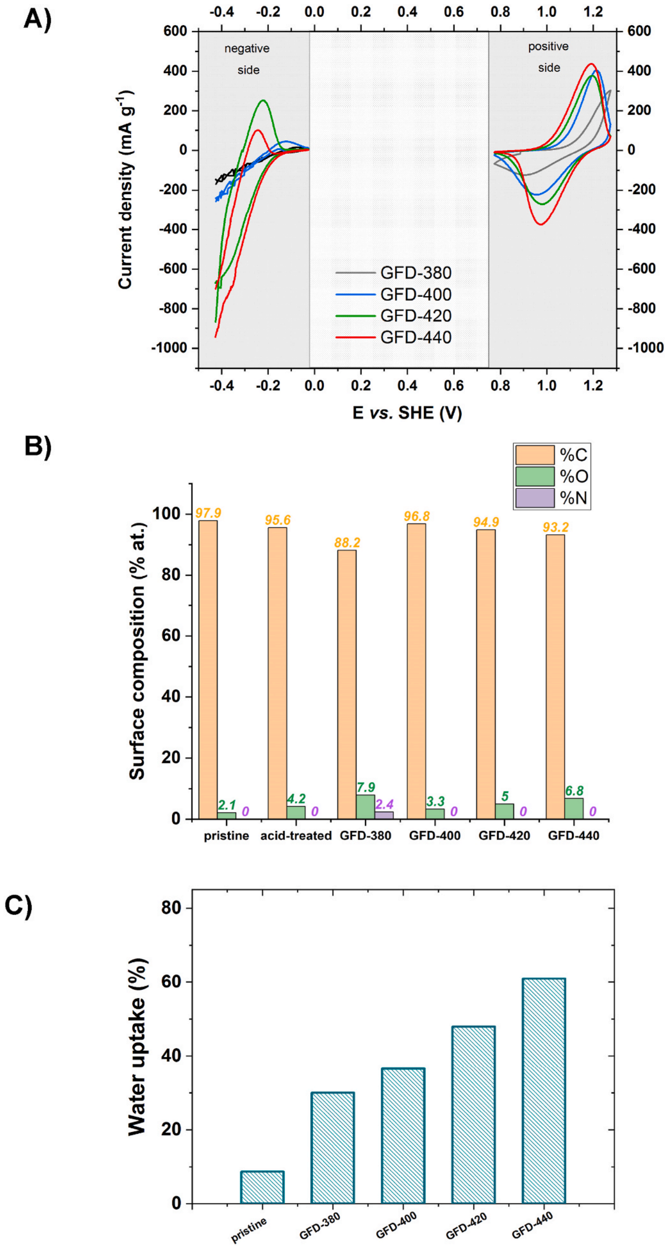

Fig. 6. GFD-based samples: A) cyclic voltammograms at 2 mV s^{-1}; B) surface composition from XPS measurements; C) water uptake. (A colour version of this figure can be viewed online.)

analysis was performed for 3–12 HT + ST samples (Fig. 11). Importantly, one may observe that the temperature increase to 500 °C allowed nitrogen to be introduced to the carbon structure. Its content increases upon treatment time from 1.5 at. % to 2.5 at.%. Similar behavior is observed for oxygen. 8 at. % of oxygen is the most appropriate content to improve the vanadium reaction for VRFB application. 3 h of carbon felt oxidation with nitrate salt presence ensures the trade-off between oxygen content (8 at. %) as well as allows small amount of nitrogen (1.5 at. %) to be introduced.

In order to prove our previous statement that 3 h of oxidation at 500 °C with salt presence (3 h HT + ST) is the most appropriate one, long-term measurements were performed. Additionally, the samples treated with salt were compared with standard heat treatment procedure. For this reason, 12 h at 500 °C has been selected since it is a usual carbon felt treatment for industrial application. The samples oxidized for 12 h with (12 h HT + ST) and without nitrate salt (12 h HT) were compared. Additionally, the most promising result, i.e., 3 h HT + ST is shown. Fig. 12 A-C presents the electrochemical responses for these carbon felts taking into account their stability.

When the 12 h HT sample is considered, one may observe that the

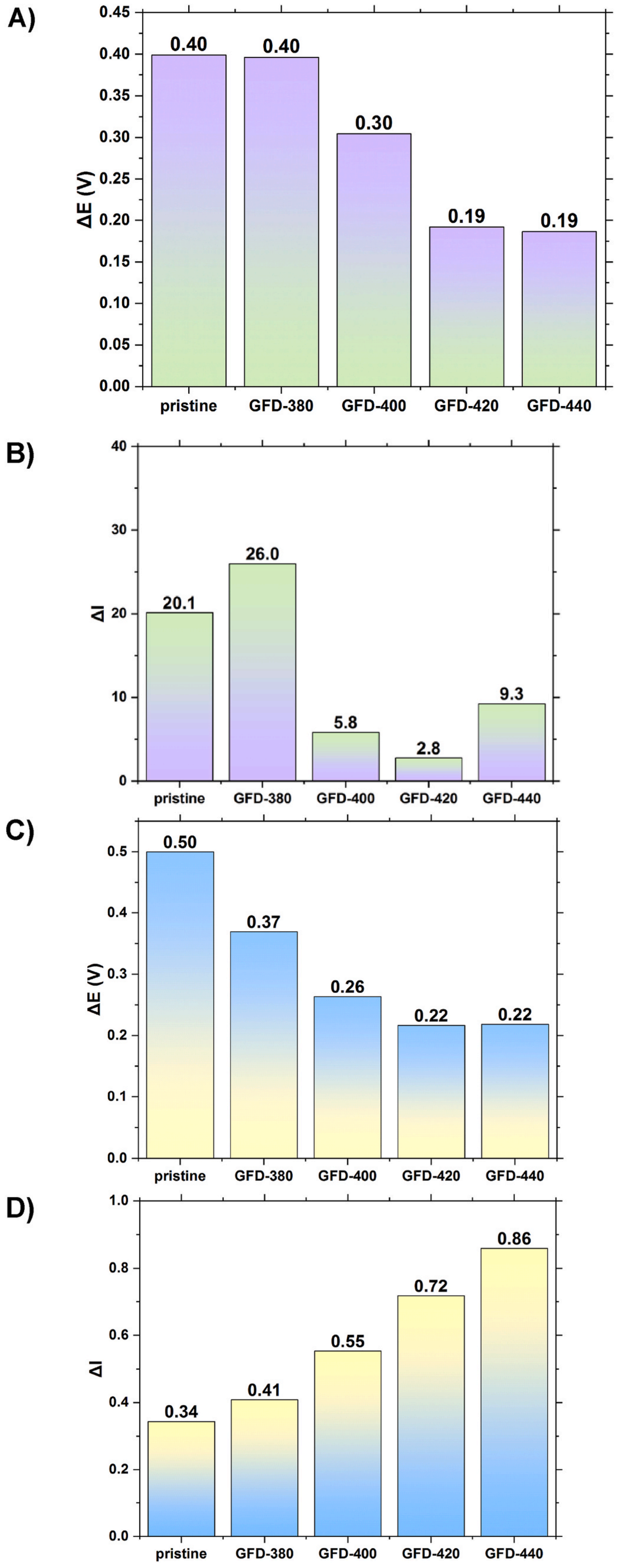

Fig. 7. Peak analysis data for GFD samples: A) and B) V^{2+}/V^{3+}; C) and D) VO^{2+}/VO_2^+ pair. (A colour version of this figure can be viewed online.)

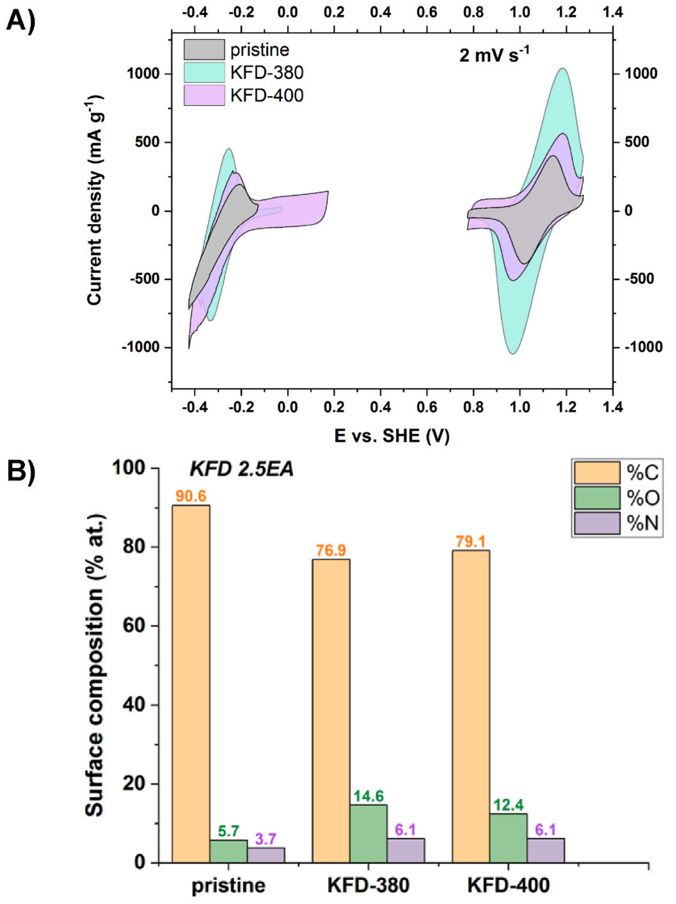

Fig. 8. KFD carbon felt: A) cyclic voltammograms at 2 mV s-1; B) electrode surface composition from XPS measurements. (A colour version of this figure can be viewed online.)

Table 2

Peak analysis for KFD carbon felt: A) V^{2+}/V^{3+}; B) VO^{2+}/VO_2^+ side.

Sample	V^{2+}/V^{3+}		VO^{2+}/VO_2^+	
	ΔE (V)	ΔI	ΔE (V)	ΔI
pristine	0.22	3.72	0.12	0.96
KFD-380	0.08	1.76	0.22	1.00
KFD-400	0.19	3.25	0.21	0.90

Table 3

Comparison of burn-off percentage for heat treated and salt treated carbon felts.

Sample	Burn-off (%)
Pristine GFD felt	0
3 h HT	1
6 h HT	1.5
12 h HT	3
3 h HT + ST	15
6 h HT + ST	57
12 h HT + ST	67

current response is relatively low. For VO^{2+}/VO_2^+ redox pair a satisfactory reversibility of redox processes is recorded as the peaks do not change over 100 cycles. However, for V^{2+}/V^{3+} pair, the CV curve becomes narrower over the cycles meaning that there is an electrode performance fade. It is herein assumed that the oxygen content is too low (4.5 at. %) to ensure stable and reversible vanadium reaction behavior.

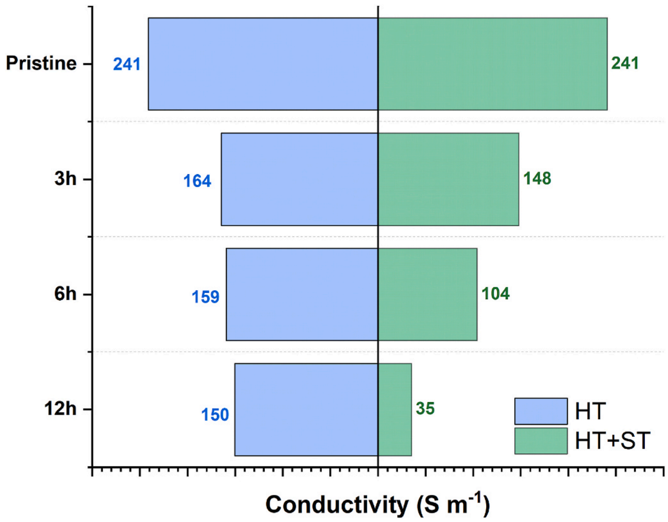

Fig. 9. Conductivity of GFD carbon felt samples upon heat and salt treatment. (A colour version of this figure can be viewed online.)

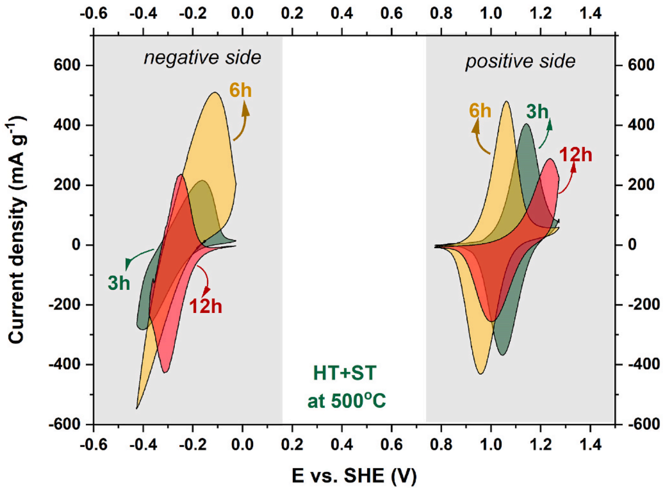

Fig. 10. Cyclic voltammograms (2 mV s^{-1}) for 3–12 h HT + ST carbon felt electrodes. (A colour version of this figure can be viewed online.)

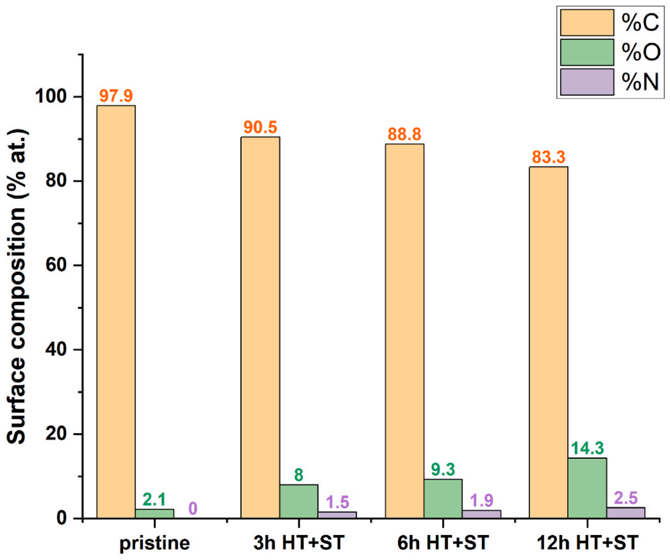

Fig. 11. Chemical composition of salt treated GFD carbon felts (500 °C) at various time (3–12 h). (A colour version of this figure can be viewed online.)

When the same conditions of electrode oxidations were utilized for CF, however, with salt presence (12 h HT + ST – Fig. 12B), the current response increased ca. 3-fold meaning that through oxidation process the CF became more active in vanadium solution. Importantly oxygen content increased to 14.3 at.% with simultaneous incorporation of nitrogen to carbon structure (2.5 at.%). When VO^{2+}/VO_2^+ redox pair is considered, relatively good reversibility is observed with negligible changes over 100 cycles. Interestingly, for negative side (V^{2+}/V^{3+}) significant vanadium peaks are formed, however, one can see that the sample was not able to further operate after 25th cycle. It is therefore assumed that the sample is overoxidized. Therefore, the last consideration is directed towards shortened time of oxidation, i.e., 3 h with salt presence (3 h HT + ST). The results presented in Fig. 12C clearly show the redox peaks for both positive and negative side. Very sharp peaks are recorded for VO^{2+}/VO_2^+ redox pair meaning that the redox processes are very reversible. The sample treated at 3 h HT + ST is very stable for positive and negative side over 100 cycles. Especially, for the V^{2+}/V^{3+} there is no evidence of hydrogen evolution which sometimes becomes a dominant reaction leading to the pH change and performance loss over time. Fig. 12D displays elemental surface composition (C, O, N) of differently treated GFD carbon felts. Evidently, nitrogen was incorporated to the carbon structure when the nitrate salt was coupled with heat treatment. Its impact is especially important for stable operation of negative side of VRFB as well as its long-term operation.

Summarizing, a good reversibility of vanadium redox processes is recorded for 3 h HT + ST samples. Moreover, nitrogen was detected on GFD carbon felt surface. Its presence significantly affects vanadium redox reaction behavior due to the improved hydrophilicity of the sample. As seen, with an extended time and at higher temperature GFD carbon felt is more sensitive to KNO_3, therefore it was necessary to increase the temperature from 440 °C to 500 °C to incorporate nitrogen to GFD structure. Graphitized carbon felt (GFD) has more rigid structure and its modification required more aggressive conditions than for carbonized felt (KFD) which was not resilient enough at high temperatures. The mechanism of the oxidation is based on nitrate salt reduction over treatment while carbon undergoes oxidation.

3.1. VRFB study including electrode polarization measurements

The VRFB performance over charging/discharging cycles operating with the GFD felts heated with and without salt at 500 °C for 3–12 h is shown in the Supporting Information (Fig. S1 A-E). The sample 12 h HT + ST is excluded from this test as the treatment resulted in very fragile electrode with too small sample dimensions resulting in poor contact with the bipolar plate.

Fig. 13 summarizes the discharge capacity per cycle at different current densities for all studied materials. There is a low constant capacity decay per cycle mainly attributed to the cross-over through the membrane. Discharge capacity also decreases with increasing current density and the drop is generally more drastic for the heat-treated samples, i.e., for 3 h HT and 6 h HT. As the activation overpotential increases with the current density, therefore, cut-off values for charge and discharge are reached earlier and the charged (or discharged) capacity is lower. In fact, the cycling at 100 mA cm^{-2} was not possible within the defined cut-off voltages for 3 h HT and 6 h HT due to high overpotential that would be required to obtain that current density. Fig. 13 reveals that the best performance is obtained for 3 h HT + ST and 12 h HT samples, suggesting a lower polarization of these electrodes. These results are confirmed by the overpotentials measurements obtained with the set-up described in Fig. 1. When comparing the only heat-treated samples, 3 h HT and 6 h HT, 6 h HT performs better at low current densities but worse at higher currents. However, these samples clearly present a worse performance when compared with the salt

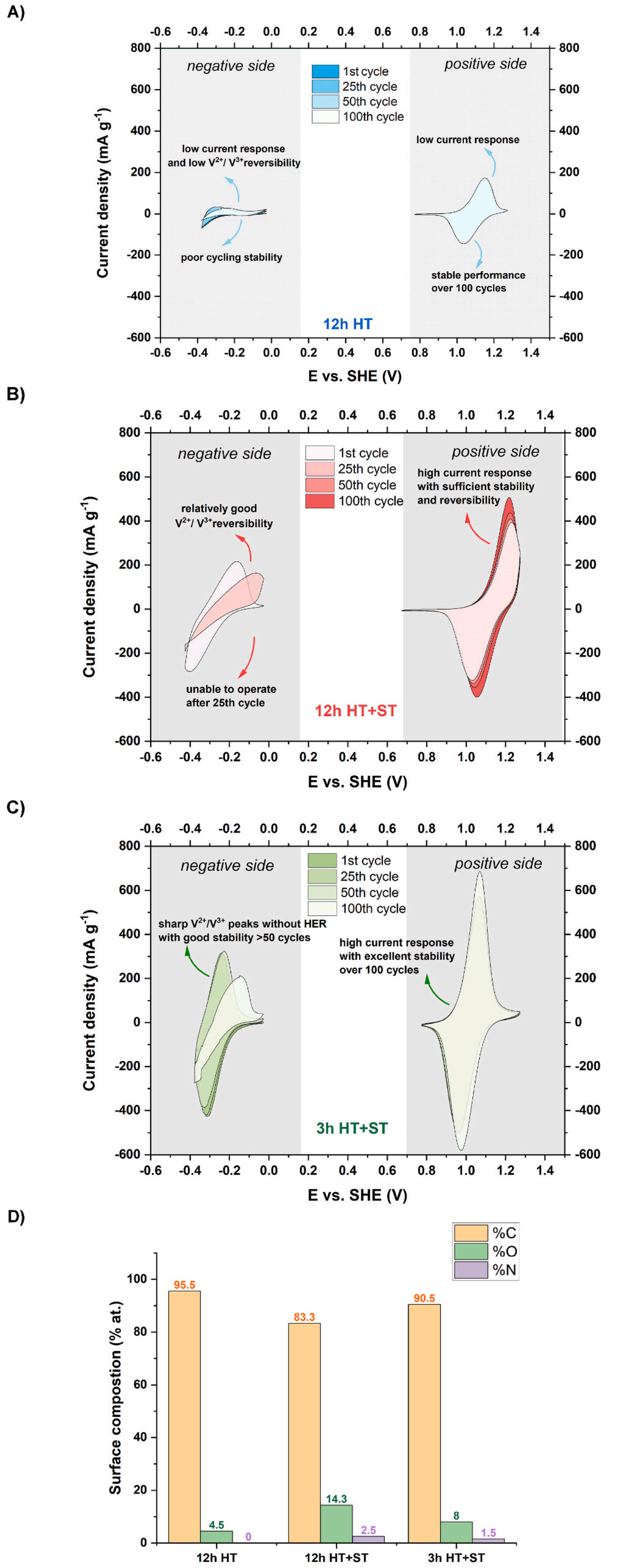

Fig. 12. GFD carbon felt at 500 °C: A) CV (2 mV s^{-1}) for heat-treated (HT) sample for 12 h; B) CV (2 mV s^{-1}) for heat & salt treated (HT + ST) sample for 12 h; C) CV (2 mV s^{-1}) for heat & salt treated (HT + ST) sample for 3 h; D) comparison of surface composition from XPS studies. (A colour version of this figure can be viewed online.)

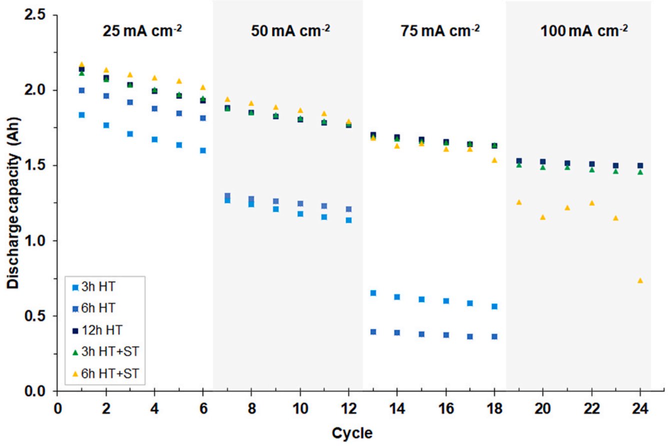

Fig. 13. VRFB discharge capacity per cycle for HT and HT + ST GFD samples. (A colour version of this figure can be viewed online.)

treated ones. 6 h HT + ST treated sample shows best discharge capacity at lower currents, but the performance becomes worse than the other two samples at 100 mA cm^{-2}.

A similar analysis can be done by studying the energy efficiency (% EE) of the battery; less polarized electrodes lead to higher efficiencies. Fig. 14 shows a significant improvement for the salt-treated samples, i. e., 3 h HT + ST and 6 h HT + ST compared with the just heated ones. Interestingly, the best performance of the battery is achieved with the long heat treatment (12 h HT). The 3 h HT + ST sample shows a similar high performance to 12 h HT sample, supporting the previous results presented within this work. It is also worth observing that the performance of 6 h HT + ST electrodes is much worse than for 3 h ST + HT. It can explain the fact that 12 HT + ST sample was overoxidized and not proper for long-term measurements on bipolar plates. It means that the optimal treatment time with salt presence is 3 h. When this time is extended a performance loss is observed.

Finally, the measurements of the electrode's polarization enable analyzing the impact that each electrode has to the overall overpotential separately. Overpotentials are changing as the battery is being charged/discharged, mostly in the extreme state of charges where mass transfer effects become more important. However, it is possible to take a stable value from the middle of the charging and discharging processes, and make a suitable comparison of the different felts. As it is difficult to define a value for the high current rates, just the two lowest current densities are analyzed here. Fig. 15A and B show the measured overpotentials of positive and negative electrodes respectively, for both

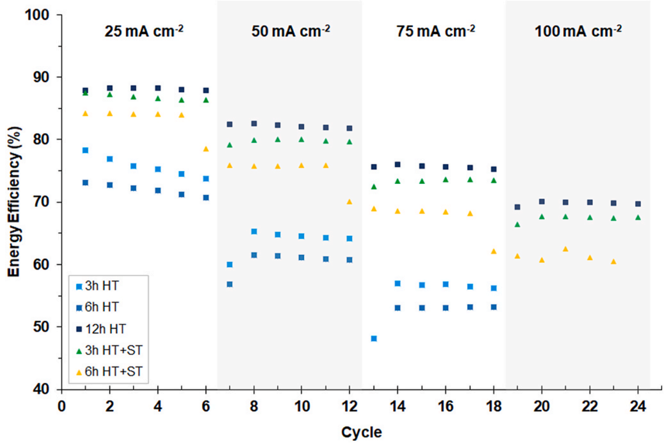

Fig. 14. VRFB energy efficiency per cycle for HT and HT + ST GFD samples. (A colour version of this figure can be viewed online.)

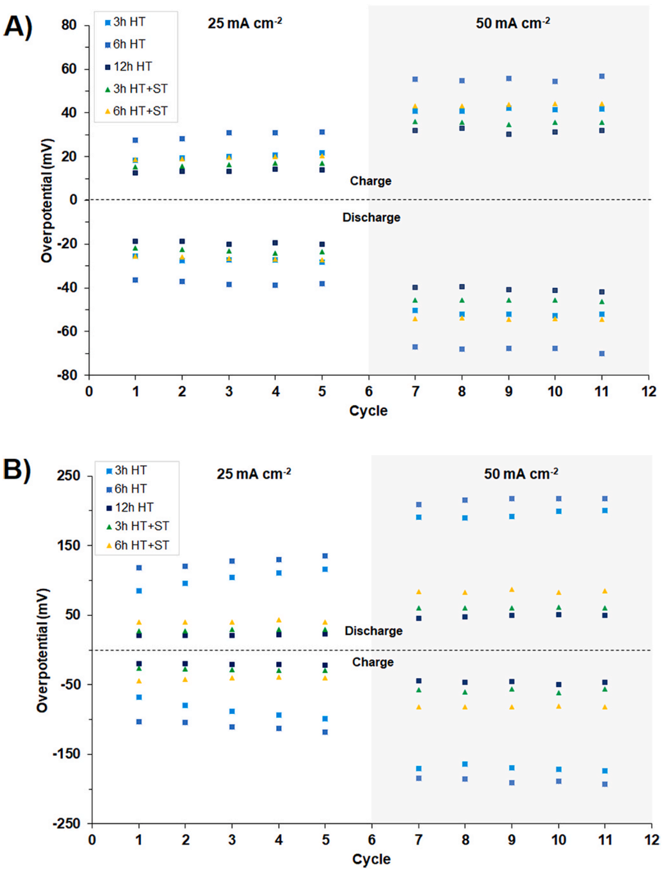

Fig. 15. Measured overpotentials per cycle for HT and HT + ST GFD samples operating as A) positive electrode; B) negative electrode. (A colour version of this figure can be viewed online.)

charge and discharge processes during the battery cycling.

The measured electrode overpotentials support the results obtained from the main cell, evidencing lower overpotentials for the salt-treated samples on both negative and positive side. As expected, the 12 h HT and 3 h HT + ST samples are the ones presenting the lowest overpotentials leading to higher performance in the battery.

In addition, Fig. 15 shows that the poor performance of the 3 h and 6 h HT electrodes results mainly from the sluggish reaction rate at the negative electrode, which requires much higher overpotentials compared with the positive side. Furthermore, it demonstrates that the salt treatment can enhance the performance of the carbon felts with a higher impact on the negative electrode, which is in accordance with the long-term measurements performed with three-electrode set-up. Fig. 15A shows that the required overpotential in the positive electrode for the sample 3 h HT is 20 and 40 mV for 25 and 50 mA cm^{-2} respectively; for the sample including the salt treatment, 3 h HT + ST, the overpotentials are 16 and 35 mV. This indicates a 15–20 % reduction of the overpotential on the positive electrode when the salt treatment is considered. When considering the same samples working on the negative side, 3 h HT requires 100 mV and 195 mV, for 25 and 50 mA cm^{-2} respectively; while 3 h HT + ST sample requires 29 and 60 mV. That means a 70 % reduction of the overpotential on the negative side for the salt treated sample. A similar improvement is observed for the 6 h treated samples. These results are in agreement with the previous studies, showing that the salt treatment can enhance the activity of the carbon felts towards vanadium redox reactions and demonstrating that the 3 h salt treated sample can achieve the same high performance as a longer 12 h heat treatment.

Finally, the results obtained from the impedance spectroscopy measurements match the carbon felt conductivity measurements discussed previously (Fig. 9). Fig. 16 shows the Nyquist plots of the main cell using the heat- and chemically-treated electrodes. Fig. 16 presents the high frequency points as this study is limited to analyze the internal resistance of the battery, which can be read from the intersection with the real axis (x-axis). These measurements were performed before starting the cycling (fresh electrolyte) and changes on the internal resistance are only attributed to the electrodes with different treatments. For the heat-treated samples, the internal resistance of the battery changes slightly with the treatment time, in agreement with the small changes on the felts' conductivity. The conductivity of the chemically treated sample (3 h HT + ST) is comparable with the heat-treated samples, however longer oxidation time in presence of the salt drastically reduces the conductivity leading to higher battery internal resistance. This indicates that high resistivity of 6 h HT + ST electrode results in higher iR losses and worse performance at increased current densities.

To summarize, the feasibility of implementing molten salt treatment using potassium nitrate as the oxidizing agent in an industrial setting, as an alternative to conventional heat-treatment methods for carbon felt electrodes, presents an intriguing avenue for enhancing electrode performance and tailoring material properties. Molten salt treatment provides a controlled environment in which potassium nitrate can efficiently introduce oxygen into the carbon felt structure, enabling targeted modifications. This level of control allows the fine-tuning of electrical conductivity and wettability of the carbon felt electrode, significantly affecting the performance of VRFBs. Furthermore, the use of potassium nitrate reduces the oxidation time by a factor of four, minimizing the heat-related costs generated by the furnace. Importantly, the presence of potassium nitrate allows nitrogen surface groups to be introduced on the carbon felt surface. Nitrogen content plays a crucial role, especially on the negative side of VRFB, where one of the main challenges is the hydrogen evolution process. This process can alter the pH in the vanadium redox flow battery electrolyte, leading to salt precipitation and changes in vanadium concentration, ultimately resulting in energy losses. Therefore, the improvement and stabilization of the carbon felt electrode over numerous charging and discharging cycles lead to a more stable shelf-life for VRFBs in real applications. Furthermore, the stability of potassium nitrate at high temperatures makes it suitable for industrial-scale applications that require elevated heat treatment conditions. However, it is crucial to recognize the need for safety measures and waste management protocols when working with potassium nitrate in a molten salt context. It is also worth emphasizing that very often innovative methods of electrode oxidation have no real chance of being utilized in industry due to the price of the materials used or too advanced preparation technique. This carbon modification is a relatively inexpensive and easy oxidation method which might have the future in real industrial processes.

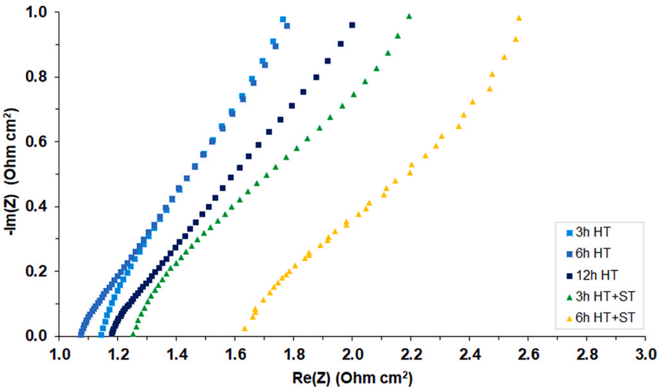

Fig. 16. Nyquist plots from electrochemical impedance spectroscopy measured on the main cell before cycling, using the HT and HT + ST GFD samples as electrode material. (A colour version of this figure can be viewed online.)

4. Conclusions

A simple molten salt oxidation method using potassium nitrate in the molten state was successfully elaborated for carbon felt treatment. Differently prepared carbon felt materials were broadly studied; their electrochemical properties were correlated with carbon surface properties. It was proven that application of relatively cheap, mild oxidizing agent, i.e., alkali metal salt (nitrate) can be competitive to previously proposed methods.

- Alkali metal salt in molten state (KNO_3) can be used as inexpensive and easily available oxidizing agent for carbon felt (CF) electrodes in VRFB. An improved vanadium reaction behaviour was recorded. Optimal treatment conditions were found for this purpose allowing the electrode preparation time to be decreased by a factor of 4.
- However, prior to the oxidation, it is recommended to pre-activate CF surface *via* immersion in HNO_3.
- Carbonized CF (KFD 2.5 EA) is more sensitive to molten salt treatment. It is thermally stable up to 400 °C with salt presence.
- Temperature increase to 500 °C for graphitized CF (GFD 4.6 EA) allowed nitrogen functional groups to be introduced to the carbon matrix; hydrophilicity increased dramatically as well as vanadium reaction is stable over 100 cycles.
- The obtained three-electrode set-up results were confirmed insightfully in the VRFB full system. The salt-treatment for GFD carbon felt clearly improved the performance of the battery as it is evidenced on the analysis of key parameters as energy efficiency.
- The overpotential measurements confirmed that the low performance of the heated samples (3 h HT and 6 h HT) results mainly from the sluggish reaction rate at the negative electrode. The performance of the GFD felts can be highly improved by application of the nitrate salt for oxidation process, increasing the redox activity towards vanadium reactions on both sides, especially on the negative electrode.
- Coupling the heat-treatment with nitrate salt as the oxidizing agent allowed nitrogen to be introduced into the carbon structure.
- The best battery performance was achieved with the samples 3 h HT + ST and 12 h HT. Evidently, nitrate salt can reduce the treatment time by factor of four holding the same high performance of VRFB.

CRediT authorship contribution statement

Justyna Piwek: Investigation, Methodology, Validation, Funding acquisition, Writing – original draft. **Gabriel Gonzalez:** Investigation, Validation, Writing – original draft. **Pekka Peljo:** Conceptualization, Supervision, Funding acquisition, Writing – review & editing. **Elzbieta Frackowiak:** Conceptualization, Supervision, Writing – review & editing.

Declaration of competing interest

The authors declare that they have no known competing financial interests or personal relationships that could have appeared to influence the work reported in this paper.

Acknowledgement

J.P. and E.F. would like to acknowledge the National Science Centre, Poland (project no. 2018/29/N/ST4/01055) for the financial support of the research.

J. P. is supported by the Foundation for Polish Science (FNP) in the framework of the START 2022 Programme.

P.P and G.G. would like to acknowledge the EU’s Horizon 2020 research and innovation programme, under grant agreement No. 875565 (CompBat project).

Appendix A. Supplementary data

Supplementary data to this article can be found online at https://doi.org/10.1016/j.carbon.2023.118483.

References

[1] A.Z. Weber, M.M. Mench, J.P. Meyers, P.N. Ross, J.T. Gostick, Q. Liu, Redox flow batteries: a review, J. Appl. Electrochem. 41 (10) (Oct. 2011) 1137–1164, https://doi.org/10.1007/s10800-011-0348-2.

[2] Á. Cunha, J. Martins, N. Rodrigues, F.P. Brito, Vanadium redox flow batteries: a technology review, Int. J. Energy Res. 39 (7) (Jun. 2015) 889–918, https://doi.org/10.1002/er.3260.

[3] G. Kear, A.A. Shah, F.C. Walsh, Development of the all-vanadium redox flow battery for energy storage: a review of technological, financial and policy aspects, Int. J. Energy Res. 36 (11) (Sep. 2012) 1105–1120, https://doi.org/10.1002/er.1863.

[4] H. Zhang, H. Zhang, X. Li, J. Zhang, Redox Flow Batteries, CRC Press, 2017, https://doi.org/10.1201/9781315152684.

[5] M. Skyllas-Kazacos, M. Rychcik, R.G. Robins, A.G. Fane, M.A. Green, New all-vanadium redox flow cell, J. Electrochem. Soc. 133 (5) (May 1986) 1057–1058, https://doi.org/10.1149/1.2108706.

[6] S. Zhong, C. Padeste, M. Kazacos, M. Skyllas-Kazacos, Comparison of the physical, chemical and electrochemical properties of rayon- and polyacrylonitrile-based graphite felt electrodes, J. Power Sources 45 (1) (May 1993) 29–41, https://doi.org/10.1016/0378-7753(93)80006-B.

[7] V. Haddadi-Asl, M. Kazacos, M. Skyllas-Kazacos, Carbon–polymer composite electrodes for redox cells, J. Appl. Polym. Sci. 57 (12) (Sep. 1995) 1455–1463, https://doi.org/10.1002/app.1995.070571205.

[8] M. Kazacos, M. Skyllas-Kazacos, Performance characteristics of carbon plastic electrodes in the all-vanadium redox cell, J. Electrochem. Soc. 136 (9) (Sep. 1989) 2759–2760, https://doi.org/10.1149/1.2097588.

[9] M. Skyllas-Kazacos, F. Grossmith, Efficient vanadium redox flow cell, J. Electrochem. Soc. 134 (12) (Dec. 1987) 2950–2953, https://doi.org/10.1149/1.2100321.

[10] R. Schweiss, A. Pritzl, C. Meiser, Parasitic hydrogen evolution at different carbon fiber electrodes in vanadium redox flow batteries, J. Electrochem. Soc. 163 (9) (Jul. 2016) A2089–A2094, https://doi.org/10.1149/2.1281609jes.

[11] C.N. Sun, F.M. Delnick, L. Baggetto, G.M. Veith, T.A. Zawodzinski, Hydrogen evolution at the negative electrode of the all-vanadium redox flow batteries, J. Power Sources 248 (Feb. 2014) 560–564, https://doi.org/10.1016/j.jpowsour.2013.09.125.

[12] L. Eifert, Z. Jusys, R.J. Behm, R. Zeis, Side reactions and stability of pre-treated carbon felt electrodes for vanadium redox flow batteries: a DEMS study, Carbon 158 (Mar. 2020) 580–587, https://doi.org/10.1016/j.carbon.2019.11.029.

[13] V. Pasala, J.N. Ramavath, C. He, V.K. Ramani, K. Ramanujam, N- and P-co-doped graphite felt electrode for improving positive electrode chemistry of the vanadium redox flow battery, ChemistrySelect 3 (30) (Aug. 2018) 8678–8687, https://doi.org/10.1002/slct.201801446.

[14] H. Yang, C. Fan, Q. Zhu, Activated charcoal modified graphite felts using for positive electrodes of vanadium redox flow battery, J. Electrochem. Energy Convers. Storage 14 (4) (Nov 2017), https://doi.org/10.1115/1.4037532.

[15] R.K. Gautam, M. Kapoor, A. Verma, Tactical surface modification of a 3D graphite felt as an electrode of vanadium redox flow batteries with enhanced electrolyte utilization and fast reaction kinetics, Energy Fuels 34 (4) (Apr. 2020) 5060–5071, https://doi.org/10.1021/acs.energyfuels.0c00701.

[16] D.O. Opar, R. Nankya, J. Lee, H. Jung, Three-dimensional mesoporous graphene-modified carbon felt for high-performance vanadium redox flow batteries, Electrochim. Acta 330 (Jan. 2020), 135276, https://doi.org/10.1016/j.electacta.2019.135276.

[17] T.X. Huong Le, M. Bechelany, M. Cretin, Carbon felt based-electrodes for energy and environmental applications: a review, Carbon 122 (Oct. 2017) 564–591, https://doi.org/10.1016/j.carbon.2017.06.078.

[18] L. Eifert, R. Banerjee, Z. Jusys, R. Zeis, Characterization of carbon felt electrodes for vanadium redox flow batteries: impact of treatment methods, J. Electrochem. Soc. 165 (11) (Aug. 2018) A2577–A2586, https://doi.org/10.1149/2.0531811jes.

[19] S. Zhong, C. Padeste, M. Kazacos, M. Skyllas-Kazacos, Comparison of the physical, chemical and electrochemical properties of rayon- and polyacrylonitrile-based graphite felt electrodes, J. Power Sources 45 (1) (May 1993) 29–41, https://doi.org/10.1016/0378-7753(93)80006-B.

[20] S. Abbas, H. Lee, J. Hwang, A. Mehmood, H.J. Shin, S. Mehboob, J.Y. Lee, H.Y. Ha, A novel approach for forming carbon nanorods on the surface of carbon felt electrode by catalytic etching for high-performance vanadium redox flow battery, Carbon 128 (Mar. 2018) 31–37, https://doi.org/10.1016/j.carbon.2017.11.066.

[21] B. Liu, S. Liu, Z. He, K. Zhao, J. Li, X. Wei, R. Huang, Y. Yang, Improving the performance of negative electrode for vanadium redox flow battery by decorating bismuth hydrogen edetate complex on carbon felt, Ionics 25 (9) (Sep. 2019) 4231–4241, https://doi.org/10.1007/s11581-019-02988-5.

[22] S. Zhong, C. Padeste, M. Kazacos, M. Skyllas-Kazacos, Comparison of the physical, chemical and electrochemical properties of rayon- and polyacrylonitrile-based graphite felt electrodes, J. Power Sources 45 (1) (May 1993) 29–41, https://doi.org/10.1016/0378-7753(93)80006-B.

[23] D.S. Aaron, Q. Liu, Z. Tang, G.M. Grim, A.B. Papandrew, A. Turhan, T. A. Zawodzinski, M.M. Mench, Dramatic performance gains in vanadium redox flow

batteries through modified cell architecture, J. Power Sources 206 (May 2012) 450–453, https://doi.org/10.1016/j.jpowsour.2011.12.026.

[24] B. Sun, M. Skyllas-Kazacos, Modification of graphite electrode materials for vanadium redox flow battery application—I. Thermal treatment, Electrochim. Acta 37 (7) (Jun. 1992) 1253–1260, https://doi.org/10.1016/0013-4686(92)85064-R.

[25] L. Eifert, R. Banerjee, Z. Jusys, R. Zeis, Characterization of carbon felt electrodes for vanadium redox flow batteries: impact of treatment methods, J. Electrochem. Soc. 165 (11) (Aug. 2018) A2577–A2586, https://doi.org/10.1149/2.0531811jes.

[26] K.J. Kim, Y.J. Kim, J.H. Kim, M.S. Park, The effects of surface modification on carbon felt electrodes for use in vanadium redox flow batteries, Mater. Chem. Phys. 131 (1–2) (Dec. 2011) 547–553, https://doi.org/10.1016/j.matchemphys.2011.10.022.

[27] R. Schweiss, A. Pritzl, C. Meiser, Parasitic hydrogen evolution at different carbon fiber electrodes in vanadium redox flow batteries, J. Electrochem. Soc. 163 (9) (Jul. 2016) A2089–A2094, https://doi.org/10.1149/2.1281609jes.

[28] I. Derr, M. Bruns, J. Langner, A. Fetyan, J. Melke, C. Roth, Degradation of all-vanadium redox flow batteries (VRFB) investigated by electrochemical impedance and X-ray photoelectron spectroscopy: Part 2 electrochemical degradation, J. Power Sources 325 (Sep. 2016) 351–359, https://doi.org/10.1016/j.jpowsour.2016.06.040.

[29] A.M. Pezeshki, R.L. Sacci, G.M. Veith, T.A. Zawodzinski, M.M. Mench, The cell-in-series method: a technique for accelerated electrode degradation in redox flow batteries, J. Electrochem. Soc. 163 (1) (2016) A5202–A5210, https://doi.org/10.1149/2.0251601jes.

[30] I. Derr, M. Bruns, J. Langner, A. Fetyan, J. Melke, C. Roth, Degradation of all-vanadium redox flow batteries (VRFB) investigated by electrochemical impedance and X-ray photoelectron spectroscopy: Part 2 electrochemical degradation, J. Power Sources 325 (Sep. 2016) 351–359, https://doi.org/10.1016/j.jpowsour.2016.06.040.

[31] I. Derr, A. Fetyan, K. Schutjajew, C. Roth, Electrochemical analysis of the performance loss in all vanadium redox flow batteries using different cut-off voltages, Electrochim. Acta 224 (Jan. 2017) 9–16, https://doi.org/10.1016/j.electacta.2016.12.043.

[32] L. Eifert, R. Banerjee, Z. Jusys, R. Zeis, Characterization of carbon felt electrodes for vanadium redox flow batteries: impact of treatment methods, J. Electrochem. Soc. 165 (11) (Aug. 2018) A2577–A2586, https://doi.org/10.1149/2.0531811jes.

[33] M. Schilling, L. Eifert, J.K. Köble, M. Jaugstetter, N. Bevilacqua, K.F. Fahy, K. Tschulik, A. Bazylak, R. Zeis, Investigating the influence of treatments on carbon felts for vanadium redox flow batteries, ChemSusChem (2023 Sep), https://doi.org/10.1002/cssc.202301063.

[34] S. Park, H. Kim, Fabrication of nitrogen-doped graphite felts as positive electrodes using polypyrrole as a coating agent in vanadium redox flow batteries, J. Mater. Chem. A Mater. 3 (23) (2015) 12276–12283, https://doi.org/10.1039/C5TA02674A.

[35] C. Flox, J. Rubio-García, M. Skoumal, T. Andreu, J.R. Morante, Thermo–chemical treatments based on NH3/O2 for improved graphite-based fiber electrodes in vanadium redox flow batteries, Carbon 60 (Aug. 2013) 280–288, https://doi.org/10.1016/j.carbon.2013.04.038.

[36] J.W. Lee, K.D. Mackenzie, D. Johnson, J.N. Sasserath, S.J. Pearton, F. Ren, Low temperature silicon nitride and silicon dioxide film processing by inductively coupled plasma chemical vapor deposition, J. Electrochem. Soc. 147 (4) (2000) 1481, https://doi.org/10.1149/1.1393382.

[37] D. Dixon, D.J. Babu, A. Bhaskar, H.M. Bruns, J.J. Schneider, F. Scheiba, H. Ehrenberg, Tuning the performance of vanadium redox flow batteries by modifying the structural defects of the carbon felt electrode, Beilstein J. Nanotechnol. 10 (Aug. 2019) 1698–1706, https://doi.org/10.3762/bjnano.10.165.

[38] H.J. Lee, D. Kil, H. Kim, Synthesis of activated graphite felt using consecutive post-treatments for vanadium redox flow batteries, J. Electrochem. Soc. 163 (13) (Sep. 2016) A2586–A2591, https://doi.org/10.1149/2.0531613jes.

[39] B. D`Aguanno, M. Karthik, A.N. Grace, A. Floris, Thermostatic properties of nitrate molten salts and their solar and eutectic mixtures, Sci. Rep. 8 (1) (Dec. 2018), 10485, https://doi.org/10.1038/s41598-018-28641-1.

[40] https://www.sglcarbon.com/en/markets-solutions/material/sigracell-battery-felts/.

[41] M. Ulaganathan, A. Jain, V. Aravindan, S. Jayaraman, W.C. Ling, T.M. Lim, M. P. Srinivasan, Q. Yan, S. Madhavi, Bio-mass derived mesoporous carbon as superior electrode in all vanadium redox flow battery with multicouple reactions, J. Power Sources 274 (Jan. 2015) 846–850, https://doi.org/10.1016/j.jpowsour.2014.10.176.